Global Academic and Scientific Journal of Multidisciplinary Studies (GASJMS)

Volume 4 | Issue 6, 2026 Homepage: https://gaspublishers.com/gasjms/ ISSN: 2583-8970

Mass Transfer Effect in the Treatment of Water polluted by Polycyclic Aromatic Hydrocarbons (Naphthalene, Anthracene, Phenanthrene, and Quinoline)

Alfred Daboh Yakubu, Evelyn Effi and C. N. Owabor

Department of Chemical Engineering, Federal University of Petroleum Resource, P.M.B 1221 Effurun, Delta State, Nigeria

Received: *11.05.2026* | ***Accepted:*** *01.06.2026* | ***Published:*** *02.06.2026*

***Corresponding Author:** Alfred Daboh Yakubu

DOI: *10.5281/zenodo.20507697*

Abstract **Original Research Article**

The study investigates the mass transfer effects in the treatment of water contaminated with polycyclic aromatic hydrocarbons (PAHs), focusing on naphthalene, anthracene, phenanthrene, and quinoline. These organic pollutants, derived from industrial processes and incomplete combustion of organic materials, are of significant environmental and health concern due to their persistence and toxicity. The research explores the adsorption of PAHs using zeolite as an adsorbent in batch experiments, analyzing external and internal diffusion mechanisms. Key findings indicate that external diffusion is the primary rate-limiting step in the sorption process. Various mass transfer models, including Fickian and non-Fickian diffusion models were applied to predict adsorption kinetics. The Biot number calculations suggest that external film diffusion predominantly controls the adsorption of phenanthrene, whereas internal diffusion dominates for naphthalene, anthracene, and quinoline. Furthermore, isotherm studies using Langmuir, Freundlich, and Redlich-Peterson models reveal that monolayer adsorption on a homogeneous surface best describes the adsorption of phenanthrene, anthracene, and quinoline, while naphthalene adsorption follows a more complex mechanism. The results provide valuable insights for optimizing adsorption processes in water treatment, highlighting the potential of Zeolite as an efficient and cost-effective adsorbent for PAH remediation. These findings contribute to the development of sustainable solutions for reducing PAH contamination and protecting environmental and human health.

Keywords: PAHs removal, Mass transfer, Adsorption isotherms, Mechanism and Kinetics.

1.0 INTRODUCTION

Over time, polycyclic aromatic hydrocarbons have threatened the environment and human health. Numerous studies have been conducted to determine ways to lessen the impact because of the effects on humans and the environment. They are created during several industrial operations and incomplete combustion of organic materials such as coal, crude oil, gas, and tobacco as noted by Datta, *et al.* (2023). Several fused aromatic rings, or carbon rings with

alternating double bonds, make up the class of organic molecules known as polycyclic aromatic hydrocarbons (PAHs) (Udom et al. 2023). The size and chemical structure of PAHs can vary; the most basic is two fused benzene rings, like naphthalene, while the more complex ones have four or more rings, like benzo[a]pyrene. PAHs are a major environmental and health problem because of their extensive wide presence (Odali et al. 2024). In summary, PAHs are a group of organic chemicals with multiple fused aromatic rings, primarily formed during incomplete combustion of organic materials. They are of environmental and health concern due to their widespread presence, persistence, and potential toxicity (Mahmoud et al. 2004). PAHs are highly lipophilic, meaning they dissolve more easily in oil than water, making their removal a challenging task. While activated carbon has been widely used as an adsorbent for wastewater remediation, its high cost has led scientists to explore alternative adsorbents from agricultural solid wastes, such as banana peels and coconut husks (Ashkanani et al. 2024). Various methods have been employed to remove PAHs and heavy metal contaminants from aqueous environments, including solvent extraction, membrane separation, and ion exchange filtration, a further noteworthy technique produces an electrical current in contaminated soil, which facilitates the transfer of toxins to electrodes buried beneath the soil (Rizzi et al. 2023). However, these techniques have limitations, such as incomplete removal and high energy consumption. Mass transfer plays a crucial role in chemical engineering separation processes, including adsorption, which is a time-dependent process. Understanding the mass transfer behavior associated with PAHs in water is essential for designing and operating efficient adsorption processes.

The study focuses on examining the mass transfer effect in the treatment of PAH-polluted water, comparing the outcome with previously published work, as well as analyzing and predicting the mass transfer behavior of these pollutants. These studies can be useful in restoring, cleaning, and improving the quality of water for a range of applications, such as agriculture, industrial processes, environmental protection, and drinking water supplies helping to create cleanup solutions that are efficient and sustainable and can reduce the threats that PAH contamination poses to human health and the environment. This study determined that particle diffusion, also known as external diffusion, is the sorption process's quickest way of diffusion. It also establishes whether the diffusion depends more on molecular (mass) diffusivity or film diffusion. Additionally, it assesses the likelihood of a uniform or irregular mass distribution in the transfer process of PAHs in water. And establishes whether the mode of transportation is Fickian (concentration-dependent) or non-fickian.

PAHs are highly lipophilic, meaning they have a stronger affinity for oil than water (Zhai et al. 2017). Activated carbon has been widely used for wastewater remediation, but, its high cost has led scientists to explore alternative adsorbents from agricultural waste, such as banana peels and coconut husks, which are cheaper and more accessible, (Lewoyehu 2021; Zhai et al. 2017). Various methods, including solvent extraction, membrane separation, and ion exchange filtration, have been used to remove PAHs and heavy metal contaminants from water. Each technique has limitations, such as incomplete removal, high energy consumption, and costly reagents (Zango et al. 2020). Agricultural waste has shown promise as a low-cost adsorbent for removing pollutants, including PAHs, from water-based environments.

Mass transfer is essential in chemical engineering separation processes, and enables the analysis of component balances. Thermodynamics dictate the feasibility and extent of separation, while mass transfer governs the rate at which separation occurs (Lakzian et al. 2024). Adsorption, a time-dependent process, is essential for removing PAHs from wastewater. Understanding the adsorption rate is vital for designing, operating, and evaluating adsorbents effectively (Odoom, Iorhemen, and Li 2024). This knowledge aids the optimization of PAH removal processes, ensuring efficient and effective wastewater treatment. According to Jaime Benitez, (Rizvi 2024) mass transfer has a profound impact on various industrial and domestic processes. The separation of mixtures relies on mass transfer between different phases, driving processes like

humidification, distillation, liquid extraction, membrane separations, adsorption, and more. The concentration gradient serves as the driving force behind these mass transfer operations, enabling the separation and transfer of components between phases.

This research extensively employs adsorption theory to investigate the mass transfer dynamics of Polycyclic Aromatic Hydrocarbons (PAHs) in water. Adsorption exploits the affinity of certain substances to bind to the surface of solids, enabling the removal of PAHs from water. The study of mass transfer in PAHs remediation and the treatment of PAHs-polluted water is crucial due to the pressing need to address the environmental and health hazards caused by PAHs contamination. The availability of relevant data highlights the significance of this research, which has the potential to yield valuable insights for environmental, social, and regulatory benefits.

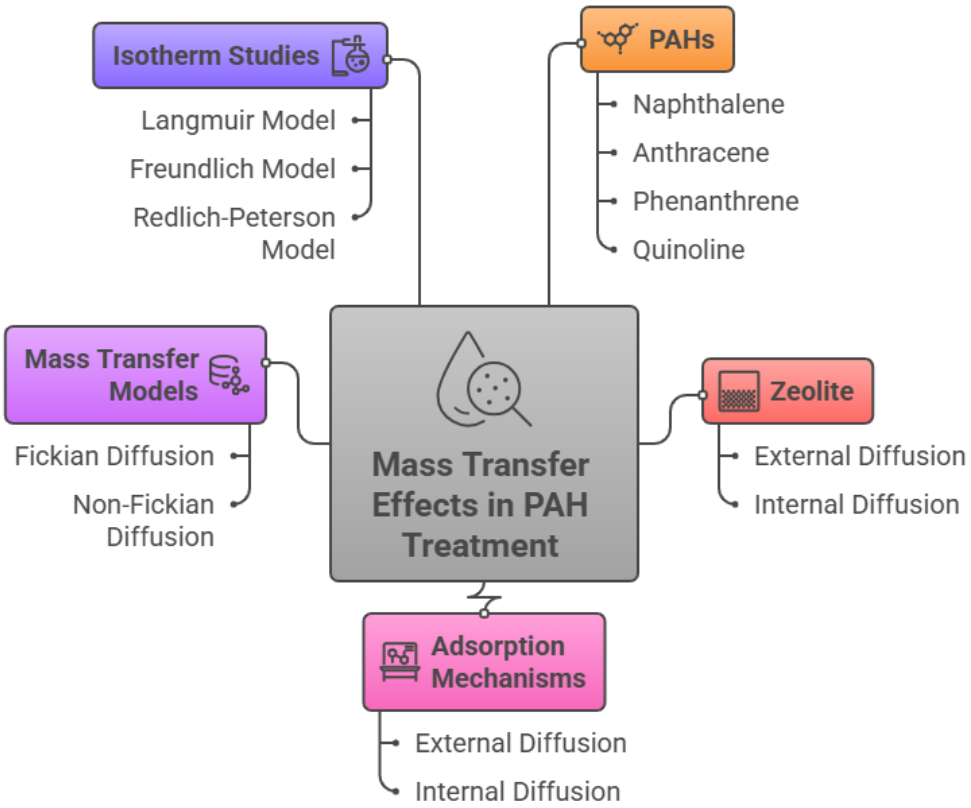

Figure 1: Mass Transfer Mechanisms Governing PAH Adsorption and Treatment in Water

2.0 MATERIALS AND METHODS

2.1 Polycyclic aromatic hydrocarbons

The PAHs used for this study were naphthalene, anthracene, phenanthrene, and quinoline, purchased from Sigma-Aldrich with a minimum assay of 99%. They purchased from were taken to the University Central Laboratory of Umaru Musa Yar'adua

University, Katsina, for detailed analysis.

2.1.1 Chemicals/reagents

Ethanol with a boiling point of 78 °C and 99% alcohol strength and distilled water were used for sample preparation and dilution, acquired from Steve More Nigeria Limited, in Zaria, Kaduna State. The Zeolite used as an adsorbent was obtained from Sigma-Aldrich. The chemicals and reagents used in the laboratory were of analytical grade and met all regulatory and compliance standards for their intended use.

2.2 Preparation and characterization of the Zeolite

The preparation of zeolite, and especially clinoptilolite and synthetic zeolite Na-X, for the removal of polycyclic aromatic hydrocarbons (PAHs) from aqueous solutions, the zeolite was synthesized and treated, possibly with NaCl, to improve its adsorption characteristics and characterized by methods such as surface area, pore size, and chemical composition, which are then used to demonstrate that the zeolites can effectively reduce the concentration of PAHs in water (with removal capacities of 0.63 to 0.68 mg g^{-1}, as reported in the literature).

Table 1: The Equipment and Apparatus used include

Equipment/Apparatus	Model	Function/Use
Mechanical Agitator	THZ-82	For homogeneous mixing
Weighing Balance	PM-4800	For Weighing of samples
Spectrophotometer	572N-UV/VIS	To Measure the concentration
BET Surface Analyzer	Quantachrome Nova 4220e	Surface area and porosity analysis
Sieve (Mesh)	V8SF#100 ASTM E11	Particle size measurement
Conical Flask	Heidolph (015890960)	For mixing and heating of solutions
Measuring Cylinder	PYREX (70022100)	To measure volume of liquid
Burette	CG-010	Volume Measurement
Pipette	CG-010	Transfer a measured volume of liquid
Volumetric flask	PYREX (5660100)	To measure and transfer liquid
Stop watch	TSA-169R	For timing
Filter Paper	FILPAPER-100	To separate solid particle from liquid
Glass rod	KRDSPNPS-56ML2	For mixing chemicals
Thermometer	MA-324C	Temperature measurement
Spatula	HMA-10	To transfer sample from one system to another

Lab funnel	SEA-100C	To channel liquid and fine grained substances into containers
Pycnometer	PYREX (15123R50)	True and bulk density measurement

2.3 Experimental procedure

2.3.1 Adsorption experiments using Zeolite (Liquid) as the adsorbent

The batch experiments were conducted with Zeolite as adsorbent at room temperature and atmospheric pressure. The Zeolite was treated with a 200-ml solution containing concentrations of 10, 20, 30, 50, 100, and 200 mg/l of the adsorbate (PAHs). Each treatment was carried out in a 200-ml standard flask. 1.0 gram of Zeolite was added to the flask and placed on a mechanical agitator with a rotation speed of 170 rpm. The flask containing Zeolite was agitated for 20 minutes and 25 minutes, respectively, until equilibrium was reached. The aqueous samples were collected at regular time intervals. The concentration of adsorbates (PAH) adsorbed was measured using a UV-visible spectrophotometer. The equilibrium concentration (C_e) of each adsorbate was determined by measuring the absorbance of the solution at equilibrium. The absorbance values were then employed in calculating the equilibrium concentration using a calibration curve or other appropriate method.

2.4 Theoretical investigation

Understanding the degree of transfer of pollutant species between the bulk and surface of solid adsorbent particles and at the interface between solid adsorbent particles or liquid and solid particles is crucial in any adsorption process. The slowest of these steps will be the controlling process, as stated by (Pollice et al. 2012). Different mass transfer models and dimensionless numbers were examined to identify the step that limits the rate of mass transfer.

2.3.1 Film Diffusion Model

The diffusion process on the adsorbent's exterior and interior surfaces was investigated using Fick's equation. The initial period of the adsorption equation is given by:

$$\frac{q_t}{q_e} = 6\left(\frac{D_1}{\pi a^2}\right)^{1/2} \times t^{1/2} \qquad (1)$$

The plot of qt/qe versus $t_{1/2}$ depicts the stages of adsorption for the film diffusion, the intra particle diffusion, and the adsorption-desorption equilibrium (Loganathan et al. 2014). From these, the rate-limiting step can be calculated.

2.3.2 External Diffusion Model

In contrast, the external diffusion model proposes that the concentration at the surface of the adsorbent approaches zero or that intraparticle resistance is negligible, thus allowing intraparticle diffusion to be disregarded in the early stages of contact (Girish and Murty 2016). This model relies on Fick's laws, which describe the solute concentration in the solution as a function of the difference between solute concentrations in the solution and at the surface of the particle (Yakub et al. 2020).The change in solute concentration over time can be written as follows:

$$\frac{\partial C/C_\circ}{\partial t} = -K_f A \qquad (2)$$

Where C is the bulk liquid phase concentration of solute at any time t, Co is the initial concentration of absorbate, kf is the external mass transfer coefficient, and A is the surface area of adsorbent per unit volume of particle-free slurry (m^{-1}) and is given by:

$$A = \frac{6M}{V\partial\rho P(1-\varepsilon\rho)} \qquad (3)$$

2.3.3 Furusawa and Smith model

The effect of external mass transfer resistance on the adsorption rate was examined using the Furusawa and Smith model (Girish and Murty 2016). The mass transfer coefficient, βL (ms−1), for adsorbates at the interface between the adsorbent and the solution was determined
using:

$$\ln\left(\frac{C_t}{C_\circ} - \frac{1}{mK_L}\right) = \ln\left(\frac{mK_L}{1+mk_L}\right) - \left(\frac{1+mk_L}{mk_L}\right)\beta_L At \quad (4)$$

Where kL is a constant (L/g) and m and A are the mass and outer surface of the adsorbent particle per unit volume of particle-free slurry (g/L and m-1), respectively.

A linear plot of ln (Ct/CO−1/(1+mL)) versus t was plotted, and the coefficient βL was calculated.

2.3.4 Furusawa and Smith Model (Modified)

The proposed modified equation for external mass transfer is given by:

$$\left(\frac{1}{\frac{1+1}{mk_l}}\right)\ln\left(\frac{C_t}{C_o} - \left(1 - \frac{C_t}{C_o}\right)\right) = -KAt \quad (5)$$

The linear plot of the above equation was used to calculate the external mass transfer coefficient k. The intercept obtained in (mkL/ (1 + mkL)) must be set to zero. However, in this case, the intercept will be zero (Mahmoud et al. 2004).

2.3.5 Particle Diffusion Model

When the adsorbent is porous, intraparticle mass diffusion can be the limiting factor in the rate of adsorption (Song et al. 2016). This relationship between the adsorption capacities at different times and the equilibrium is established using:

$$\ln\left[\frac{1}{1-F^2(t)}\right] = \frac{\pi^2}{a^2} D_e t \quad (6)$$

Whereby the function; $\frac{\pi^2}{a^2} D_e t = \frac{q_t}{q_e}$

Therefore: $F_{(t)} = \frac{q_t}{q_e}$ (7)

Where: q_t and q_e are the amount of uptake at time t and equilibrium, respectively; a is the particle radius. The diffusion coefficient De is calculated by using the values obtained from the straight-line plot of $-\ln(1 - F^2(t))$ versus t from Equation 4.

2.3.6 Mass Diffusivity

The surface properties of adsorbents play a key role in determining the diffusion coefficient. To examine the diffusion coefficients for the intra-particle transport of PAHs within the pores of adsorbent particles at different concentrations, the following expression was utilized:

$$D_m = \frac{0.03a^2}{t^{1/2}} \quad (8)$$

D_m (mass diffusivity) is inversely proportional to $t^{1/2}$ (half-reaction time). Half-adsorption time, $t^{1/2}$, is defined as the time required for adsorption to take up half of what the adsorbent can take at equilibrium (Girish and Murty 2016). This time is also often used as a measure of the adsorption rate:

$$t^{\frac{1}{2}} = \frac{1}{K_2 q_e} \quad (9)$$

Where: K_2 and, q_e corresponds to the second-order rate constant and equilibrium adsorption capacity (from previous batch studies), respectively, and the value of a used in equation (8) is the particle radius. The solid phase is expected to be comprised of spherical particles with an average radius between the radii corresponding to the upper and lower size fractions.

2.3.4 Experimental parameters (kf and De) in terms of dimensionless numbers

To study the mass transfer behaviour, the experimental parameters can also be represented in terms of dimensionless groups. To investigate the rate-limiting step, the parameters were expressed in terms of the Biot (Bi) number. To demonstrate the effect of concentration on the adsorption process, an expression for the Bi number in terms of concentration was developed (Zango et al. 2020).

2.3.5 Biot Number:

The Biot (Bi) number, as illustrated below, establishes a connection between the resistance to mass transfer external to the system and the resistance within the system. It quantifies the ratio of the transport rate in the liquid layer to the intra particle mass transfer rate (Yakub et al. 2020). The Bi number serves as an important parameter in identifying the step that limits the overall rate. Its mathematical expression is provided by:

$$Bi = \frac{K_f d}{D_e} \quad (10)$$

If Bi is greater than 100, the adsorption process is primarily controlled by the external diffusion mechanism; if Bi is less than 100, the adsorption process is primarily controlled by film transfer (Yu, Ma, and Bi 2015).

3.0 RESULTS AND DISCUSSSION

3.1 Characterization of the Zeolite

The physicochemical characterization of zeolite obtained from Sigma-Aldrich was determined as described below and is listed in Table 2. Zeolites are crystalline, microporous aluminosilicate minerals with a three-dimensional framework structure made up of tetrahedra of AlO_4 and SiO_4. Physicochemical characterization of zeolites involves the determination of various properties, such as their crystal structure, true density, chemical composition, bulk density, surface area, porosity, acidity, pore volume, and thermal stability. The physicochemical characterization of zeolites is essential in understanding their properties and optimizing their use in various applications, such as catalysis, adsorption, and separation processes.

Table 1: Physicochemical Characterization of Zeolite

Physicochemical Characterization	Values
Mean particle size (mm)	0.400
Surface area (m^2/g)	74.920
Pore Size (A®)	4.000
Bulk Density (g/cm^3)	0.721
True Density (kg/m^3)	2.771
Pore Volume (cm^3/g)	0.440
Porosity (%)	0.590

Particle Size: The mean particle size of the zeolite is relatively large at 0.400 mm, suggesting the material consists of moderately sized particles. Surface Area: The reported surface area of 74.920 m²/g indicates that the zeolite possesses a significant surface area available for adsorption. This high surface area suggests it could be efficient for adsorbing molecules or ions onto its surface. Pore Size: The pore size of

4.000 Å indicates that the zeolite possesses small-sized pores, potentially suitable for trapping or adsorbing molecules or substances of specific sizes. Bulk Density: The bulk density of 0.721 g/cm³ suggests that the material, in its bulk state, has a relatively low density, indicating the presence of pore spaces within the material. True Density: The true density, reported as 2.771 kg/m³, indicates the density of the material if all the pores were completely filled. This value is significantly higher than the bulk density, indicating the presence of substantial pore space within the material (Bulk Specific Gravity, 2023). Pore Volume: The reported pore volume of 0.440cm³/g indicates the volume of pores present within the material, highlighting its porosity and the capacity to hold substances within these pores. Porosity: The reported porosity of 0.59% indicates the fraction of the total volume of the material that is occupied by pores. This suggests that a small fraction of the material's volume is actually solid, while the majority consists of pore space.

The zeolite material is well-equipped for adsorption purposes. Its impressive surface area, moderate pore size, substantial pore volume, and porosity all contribute to its suitability for this purpose. The difference between its bulk density and true density reveals the existence of a substantial amount of pore space, making it highly promising for applications that require adsorption or selective molecular trapping.

Table 3: The equilibrium concentration (q_e) of adsorbates at different concentrations.

Adsorbate	Naphthalene		Anthracene		Phenanthrene		Quinoline	
C_og/L	qe	Absorbance	qe	Absorbance	qe	Absorbance	qe	Absorbance
10	0.008	0.004	0.214	0.02	0.219	0.412	0.191	0.199
20	0.011	0.002	0.392	0.109	0.416	0.524	0.259	0.404
30	0.013	0.006	0.501	0.092	0.518	0.483	0.344	0.104
50	0.015	0.003	0.58	0.092	0.596	0.466	0.379	0.552
100	0.017	0.005	0.637	0.701	0.789	0.605	0.432	0.344
200	0.020	0.002	0.701	0.705	0.889	0.700	0.44	0.696

Table 3 provides information on the equilibrium concentration (q_e) of different adsorbates at various initial concentrations. The equilibrium concentration is a measure of the quantity of adsorbate that remains in solution once adsorption has reached equilibrium with their respective absorbance values. For each adsorbate, the initial concentrations tested range from 10 g/l to 200 g/l.The results show that the equilibrium concentration of each adsorbate increases with increasing initial concentration, but

the rate of increase varies depending on the adsorbate. Overall, the results suggest that the adsorption of these four adsorbates onto the adsorbent under study is concentration-dependent. The adsorption capacity of the adsorbent increases with increasing initial concentration, which is reflected in the increase in equilibrium concentration. The differences in the rate of increase of equilibrium concentration between the different adsorbates suggest that their adsorption behavior is also influenced by other factors such as their chemical structure and polarity.The Table provides valuable information for researchers and practitioners interested in the remediation of these adsorbates from wastewater or other aqueous solutions. The data can be used to estimate the adsorption capacity of the adsorbent under different initial concentrations of the adsorbate and optimize the design of adsorption systems.

3.2 External Mass Transfer Model

Table 4 presents mass transfer coefficients (Kf) for four adsorbates: naphthalene, anthracene, phenanthrene, and quinoline. These coefficients were determined using the external diffusion model for adsorption. The mass transfer coefficient (Kf) represents the rate of solute transfer from the bulk fluid phase to the adsorbent surface and it is influenced by various factors such as adsorbent and solute properties, solute concentration, and operating conditions (e.g., temperature, pressure, flow rate) (Yakub et al., 2020; Danish et al., 2022)

From Table 4, we can observe that the K_f decreases as the initial solute concentration increases for each adsorbate. This decrease is expected because the driving force for mass transfer decreases with higher solute concentrations (Aguilera & Gutiérrez Ortiz, 2016). Among the adsorbates, Anthracene exhibits the highest K_f values of 0.054 m/s at 10 g/L initial concentration, indicating highly efficient adsorption and less resistant to mass transfer from bulk liquid medium to the adsorbent surface while Quinoline shows the lowest K_f value of 5.60×10^{-6} m/s at 200 g/L initial concentration, suggesting less efficient adsorption. For naphthalene and anthracene, the K_f values are relatively similar and decrease slowly with increasing concentration, implying that concentration changes have a limited impact on their adsorption. However, for quinoline, the K_f values decrease more rapidly with increasing concentration, suggesting a stronger influence of concentration effects on its adsorption. This outcome suggests that the interaction between the zeolite and the Quinoline may be weaker (Huang et al., 2020) leading to difficulty diffusing through the boundary layer surrounding to the zeolite particles. Going by the data presented in Table 4, zeolite has more affinity for anthracene, followed by Naphthalene, Phenanthrene, and Quinoline. Overall, the table provides valuable insights into the adsorption behavior of different species under various conditions, aiding in the design and optimization of adsorption processes.

Table 4: Mass transfer coefficients (K_f) from the external diffusion model for the adsorption of adsorbates obtained from the equation

Adsorbate	Naphthalene		Anthracene		Phenanthrene		Quinoline	
C_og/L	R^2	k_fm/s	R^2	k_fm/s	R^2	k_fm/s	R^2	k_fm/s
10	0.999	0.00166	0.966	0.0540	0.966	0.000356	0.990	5.71×10^{-6}

20	0.967	0.00140	0.969	0.0533	0.978	0.000347	0.941	5.68×10^{-6}
30	0.984	0.00137	0.989	0.0530	0.991	0.000343	0.982	5.65×10^{-6}
50	0.987	0.00125	0.979	0.0524	0.900	0.00040	0.967	5.64×10^{-6}
100	0.999	0.00123	0.927	0.0521	0.972	0.000337	0.981	5.62×10^{-6}
200	0.988	0.0012	0.984	0.0520	0.981	0.000335	0.937	5.60×10^{-6}

Furusawa and Smith model

Table 5 displays the obtained mass transfer coefficients (B_L) using the Furusawa and Smith model for the adsorption of various adsorbates (naphthalene, anthracene, phenanthrene, and quinoline) at different initial concentrations (C_o) in aqueous solutions. The mass transfer coefficient, which is represented by B_L in Furusawa and Smith model, shows how fast the adsorbate travels from the liquid to the surface of the Zeolite (Aguilera & Gutiérrez Ortiz, 2016). The difference in concentration between the bulk liquid and the adsorbent surface is the fundamental concept behind the mass transfer mechanism in this model (Yakub et al., 2020), hence, the faster the contaminants (adsorbates) transfer to the zeolite surface, the larger the concentration difference. The rate of adsorption increases with the increase of the mass transfer coefficient, which depends on the concentration gradient. According to the Furusawa and Smith model, as the initial concentration of the adsorbate increases, the mass transfer coefficient tends to decrease, suggesting that the rate of solute adsorption slows down as the solute concentration increases, potentially due to saturation effects or reduced driving force (Danish et al., 2022; Girish & Murty, 2016). The data presented in Table 5 support this model because B_L decreases as initial concentration increases validating the outcome of the external diffusion model which states that the rate-limiting step is the movement of adsorbate particles to the surface of the zeolite.

However, in contrast to the findings of the external diffusion model, the phenanthrene contaminant appeared to be more favorably adsorbed by the zeolite with the highest B_L values of 8.6×10^{-5} m/s occurring at 10 g/L and 30 g/L initial concentrations., followed by Quinoline, 5.6×10^{-7} , Naphthalene, 7.4×10^{-7} at 10g/L concentration and Anthracene having the lowest values of $B_{L,}$ 7.3×10^{-9} m/sat 200 g/L concentration. In addition, the high values of R^2 presented in Table 5 proved that this model has a high correlation with the adsorption data. The mass transfer coefficient across all the contaminants at different concentrations obtained in the External Diffusion Model is significantly higher than that obtained by the Furusawa and Smith model. Hence, the External diffusion model is well-suited for this experiment.

Table 5: Mass transfer coefficients from the Furusawa and Smith model for the adsorption of Adsorbates obtained from equation 3.6.

Adsorbate	Naphthalene		Anthracene		Phenanthrene		Quinoline	
C_og/L	R^2	$\beta_{L\ m/s}$	R^2	$\beta_{L\ m/s}$	R^2	$\beta_{L\ m/s}$	R^2	$\beta_{L\ m/s}$
10	0.9751	7.4×10^{-7}	0.9514	8.0×10^{-9}	0.9714	8.6×10^{-5}	0.9911	5.6×10^{-7}
20	0.9800	7.0×10^{-7}	0.9601	7.8×10^{-9}	0.9813	8.4×10^{-5}	0.9641	5.3×10^{-7}
30	0.9510	6.8×10^{-7}	0.9507	7.7×10^{-9}	0.9741	8.6×10^{-5}	0.9531	5.3×10^{-7}
50	0.9407	6.5×10^{-7}	0.9601	7.5×10^{-9}	0.9814	8.3×10^{-5}	0.9712	5.1×10^{-7}
100	0.9501	6.4×10^{-7}	0.9742	7.5×10^{-9}	0.9666	8.2×10^{-5}	0.9517	5.0×10^{-7}
200	0.9601	6.2×10^{-7}	0.9804	7.3×10^{-9}	0.9541	8.1×10^{-5}	0.9583	4.8×10^{-7}

Furusawa and Smith model (modified)

Table 6 contains the obtained mass transfer coefficients (k) data using the Furusawa and Smith model for the adsorption of various adsorbates (naphthalene, anthracene, phenanthrene, and quinoline) at different initial concentrations (C_o) in aqueous solutions. The mass transfer coefficient *k* has a more expanded function in the modified Furusawa and Smith model than in the original model because it takes into account both internal and external diffusion, which is the movement of the solute within the adsorbent's pores and from the bulk fluid to the surface (Girish & Murty, 2016). Under this setting, the effective mass transfer coefficient represented by the parameter *k* usually combines these two diffusion processes, improving the model's applicability to complicated adsorption systems and porous materials.

Similar to other models discussed above, the effective mass transfer coefficient (k) decreases as the concentration increases for the four contaminants studied, confirming the validity of their outcome. Meanwhile, the effect of concentration gradient is more pronounced in the sorption of Naphthalene compared to other adsorbates as evidenced in Table 6, where the values of k change from 6.43×10^{-6} m/s at 10 g/L concentration to 3.57×10^{-6} at 200 g/L, which is approximately 50% decrease. Since k is the combined effect of both external and internal diffusion, we can deduce that the movement of Naphthalene from the liquid medium to the zeolite surface is the rate-limiting step for naphthalene adsorption while it may not be for other contaminants because changes in concentration did not significantly affect the values of k. This result agrees with (Leyva-Ramos & Geankoplis, 1985a). The highest value of 8.45×10^{-6} of k was obtained in the Anthracene adsorption process at 10 g/L, suggesting a higher affinity of the zeolite to the Anthracene contaminant compared to other contaminants.

Table *6*: Mass transfer coefficients for the adsorption of adsorbates obtained from equation 3.7. Furusawa and Smith model (modified)

Adsorbate	Naphthalene		Anthracene		Phenanthrene		Quinoline	
C_og/L	R^2	km/s	R^2	km/s	R^2	km/s	R^2	km/s
10	0.9718	6.43×10^{-6}	0.9401	8.45×10^{-6}	0.9990	5.75×10^{-6}	0.9634	6.00×10^{-6}
20	0.9613	6.31×10^{-6}	0.9400	8.17×10^{-6}	0.9751	5.54×10^{-6}	0.9601	5.72×10^{-6}
30	0.9541	4.72×10^{-6} s	0.9389	7.65×10^{-6}	0.9654	5.27×10^{-6}	0.9522	5.60×10^{-6}
50	0.9470	4.41×10^{-6}	0.9389	7.35×10^{-6}	0.9563	4.80×10^{-6}	0.9422	5.20×10^{-6}
100	0.9420	3.87×10^{-6}	0.9362	6.02×10^{-6}	0.9501	4.50×10^{-6}	0.9400	4.81×10^{-6}
200	0.9382	3.57×10^{-6}	0.9241	5.85×10^{-6}	0.9421	4.25×10^{-6}	0.9400	4.60×10^{-6}

3.3 Particle Diffusion Model

Table 7 provides information on the diffusion coefficients of different PAHs at various concentrations. The diffusion coefficient (De) represents the rate at which a substance diffuses through a medium, such as a liquid or a gas. It is expressed in square meters per second (m^2/s). Although a change in concentration affects the value of De, the effect is not uniform across the adsorbate as seen in Table 7 because each adsorbate has its optimum concentration. For instance, the optimum concentration of Naphthalene that produces the highest value of De, 7.8×10^{-6} is 100 g/L; for Anthracene, it is 20 g/L when De is 1.8×10^{-7}; for Phenanthrene, it is 30 g/L when De is 8.8×10^{-4} and for Quinoline, the optimum concentration is 50 g/L when De is 2.9×10^{-4}. The diffusion coefficient, De, has an impact on mass transfer coefficient k because diffusion usually happens through a fluid boundary layer, and the mass transfer coefficient frequently takes this layer's molecular diffusion effect into account. Among the four contaminants investigated, Phenanthrene has the highest diffusion rate, which suggests a higher mass transfer coefficient and adsorption rate. The diffusion coefficient, De and the mass transfer coefficient k are directly correlated, particularly in systems where molecular diffusion predominates as the mass transfer process (Leyva-Ramos & Geankoplis, 1985a; Wang & Guo, 2022). The mass transfer coefficient is inversely related to the thickness of the boundary layer and takes into account the effects of diffusion through a boundary layer, hence, enhancing the diffusion coefficient increases the mass transfer coefficient as well, which enhances the total mass transfer rate across the phase border (Wang & Guo, 2022).

Table 7: The values of diffusion coefficients obtained from the particle diffusion model analysis at different concentrations of adsorbates

Adsorbate	Naphthalene		Anthracene		Phenanthrene		Quinoline	
C_og/L	R^2	D_e, m^2/s	R^2	D_e, m^2/s	R^2	D_e, m^2/s	R^2	D_e, m^2/s
10	0.8502	7.7×10^{-6}	0.9698	1.6×10^{-7}	0.9266	8.6×10^{-4}	0.8452	2.6×10^{-4}
20	0.9725	5.6×10^{-6}	0.8416	1.8×10^{-7}	0.8924	7.8×10^{-4}	0.9424	1.6×10^{-4}
30	0.9462	7.4×10^{-6}	0.9631	1.5×10^{-7}	0.9515	8.8×10^{-4}	0.9121	2.8×10^{-4}
50	0.9736	7.6×10^{-6}	0.9001	4.1×10^{-7}	0.9121	8.6×10^{-4}	0.9400	2.9×10^{-4}
100	0.9649	7.8×10^{-6}	0.9011	1.6×10^{-7}	0.9616	5.9×10^{-4}	0.9190	2.7×10^{-4}
200	0.8971	7.2×10^{-6}	0.9811	1.7×10^{-7}	0.8196	6.5×10^{-4}	0.9782	2.1×10^{-4}

Mass Diffusivity Model

The diffusion coefficients derived from the mass diffusivity model analysis at various PAH concentrations are shown in Table 8. The rate at which a substance diffuses through a medium, in this case, the mass diffusivity model is represented by the diffusion coefficient (D_m). The unit of measurement is expressed in square meters per second (m^2/s). The time needed for half of a substance's initial amount to pass through a medium is indicated by the $t^{1/2}$ values.

These values are crucial for understanding how these chemicals move and spread in different environments, such as in chemical processes, transport through membranes, or other applications involving mass transfer.

Table8: The values of the diffusion coefficient obtained from the mass diffusivity model analysis at different concentrations of adsorbates

Adsorbate	Naphthalene		Anthracene		Phenanthrene		Quinoline	
C_og/L	$t^{1/2}$, s	D_m, m^2/s	$t^{1/2}$, s	D_m, m^2/s	$t^{1/2}$, s	D_m, m^2/s	$t^{1/2}$, s	D_m, m^2/s
10	1736.11	2.7×10^{-4}	8680.55	5.5×10^{-5}	4566.21	1.0×10^{-5}	4019.31	1.1×10^{-4}

20	3472.22	1.4×10^{-4}	21069.37	2.3×10^{-5}	4866.71	9.9×10^{-5}	4214.59	1.1×10^{-4}
30	8680.55	5.5×10^{-4}	2365.41	2.0×10^{-5}	4178.32	1.1×10^{-5}	5051.26	9.5×10^{-4}
50	1157.55	4.1×10^{-4}	2857.10	1.7×10^{-5}	5020.73	9.9×10^{-5}	6707.38	7.1×10^{-4}
100	1212.75	3.9×10^{-4}	1607.13	2.9×10^{-5}	7288.63	6.6×10^{-5}	8230.61	5.8×10^{-4}
200	1419.71	3.4×10^{-4}	1607.84	2.9×10^{-5}	1327.41	3.6×10^{-5}	9091.51	5.3×10^{-4}

Biot number

Table 10 provides information on the relative importance of external mass transfer resistance compared to internal mass transfer resistance for different chemicals at various concentrations. The Biot number (Bi) is a dimensionless quantity that characterizes the relative importance of external mass transfer resistance to internal mass transfer resistance (Bergman, 2011; Byron Bird et al., 2006; Cussler, 2009). If Bi is greater than 100, the adsorption process is primarily controlled by the bulk diffusion mechanism; if Bi is less than 100, the adsorption process is primarily controlled by film transfer (Yu et al., 2015). From the data presented in Table 10, all the contaminants have a Bi number less than 100 suggesting film mass transfer predominates. In addition, the diffusion within the adsorbent is substantially faster than mass transfer at the surface if the Bi<40, indicating that internal diffusion predominates and there are notable concentration gradients within the adsorbent material if Bi>40, where external or surface mass transfer predominates and the rate of diffusion within the adsorbent material is significantly slower than the surface mass transfer (Pratik, 2021). In Table 10, only Phenanthrene has Bi > 40. Hence, the external mass transfer predominates in the Phenanthrene adsorption process suggesting internal diffusion to be the rate-limiting step while the reverse is the case for Quinoline, Anthracene, and Naphthalene.

Table 9: The values of the Biot number obtained from the external diffusion model for adsorbates at different initial concentrations.

Adsorbate	**Naphthalene**	**Anthracene**	**Phenanthrene**	**Quinoline**
C_o**g/L**		**Biot Number**		
10	21.58	33.75	41.39	21.96

20	25.00	29.61	44.48	35.50
30	18.14	35.33	40.98	20.17
50	16.47	12.78	40.00	19.44
100	15.69	32.56	57.11	20.81
200	16.67	30.59	51.54	22.27

3.4 Isotherm Models

The Langmuir, Freundlich, and Redlich-Peterson isotherm model was used to study the adsorption behavior of the four contaminants in Zeolite adsorbent. Table 10 is a presentation of the values of the three isotherms parameters and Figure 1 shows the isotherm plot.

The Langmuir Isotherm Model (LIM): implies monolayer adsorption on a surface with a finite number of identical sites. R^2 is the coefficient of determination, which indicates how well the model fits the experimental data, Qm(mg/g) is the maximum adsorption capacity of the adsorbents, and K_L (mg/L) is the Langmuir constant related to the affinity of the binding sites. From Table 10, the high R^2 result (0.9931) indicates that the LIM is an excellent fit for Quinoline adsorption by the zeolite, demonstrating monolayer adsorption on a uniform surface (Yang et al., 2019; Xu et al., 2018)**.** The maximum adsorption capacity (Qm) is 0.4870 mg/g, indicating the number of active sites on the Zeolite. This suggests that 0.4870 mg/g is the maximum quantity of Quinoline that can be adsorbed on the Zeolite surface to create a monolayer. The LIM constant (K_L) of 0.0661 L/mg indicates a modest affinity for Quinoline at the adsorbent surface. Higher K_L values suggest stronger binding between the adsorbate and the adsorbent, indicating a preference for adsorption over desorption (Wu et al., 2020). Also, Table 10 reveals that the LIM of Phenanthrene has a great fit (R^2=0.9956), showing monolayer adsorption (Gupta & Singh, 2018; Xiao et al., 2015; Wu et al., 2020). The maximum adsorption capacity (Qm) of 1.0329 mg/g is higher than that of Quinoline. However, the affinity of the Zeolite adsorption site for Phenanthrene is 0.0309 L/mg, which is lower. This suggests that the zeolite adsorption sites may not be as strongly attracted to Phenanthrene (Wu et al., 2020) as they were to Quinoline. In addition, the R^2 value of 0.9895 for Anthracene contaminant indicates a good fit (Tirado-Guizar et al. 2020; El Khames Saad et al. 2014), albeit somewhat lower than Quinoline and Phenanthrene. The maximum adsorption capacity (Qm) of Zeolite for Anthracene contamination is 0.7829 mg/g, greater than Quinoline but lower than Phenanthrene. The degree of affinity (K_L) of the Zeolite sorption site for Anthracene is 0.0496 L/mg, which is lower than Quinoline but higher than Phenanthrene, indicating a moderate affinity. Furthermore, in the Naphthalene sorption process, the R^2 value of 0.9931 for Naphthalene indicates an excellent fit. However, the sorption capacity (Qm) of the Zeolite over Naphthalene is 0.0208 mg/g, which is low compared to other pollutants. The K_L value of 0.0581 L/mg is significantly greater than those for Anthracene and Phenanthrene. This result indicates that the Zeolite adsorption site has a higher affinity for Naphthalene, indicating a strong interaction between Naphthalene and Zeolite. However, LIM does not accurately describe the adsorption properties of the Zeolite sorption process over Naphthalene because the low Qm values indicate that the sorption process is not controlled by the monolayer adsorption. This outcome is agreeing with

(Wu et al., 2020).

The Freundlich Isotherm Model (FIM): analyzes adsorption on heterogeneous surfaces with a non-uniform heat distribution (Vigdorowitsch et al., 2021). R^2, K_f (mg/g), and n are the coefficients of determination, FIM constant and adsorption capacity, and adsorption intensity, respectively. If n is more than one, the adsorption process is favorable (Vigdorowitsch et al., 2021; Ogbu et al., 2023). The FIM parameter in Table 10 for Quinoline has a little lower R^2 value (0.9519) than the LIM, indicating that it is not as precise in representing the adsorption of Quinoline onto the Zeolite surface. The FIM adsorption capacity (K_f) for Quinoline is 0.1387, lower than the Qm from LIM. However, the value of n (4.292) is greater than 1, indicating high heat of adsorption and favorable adsorption (Thomas et al., 2010) on a heterogeneous surface and the lower R^2 value suggests that surface heterogeneity is not significant in this case. Additionally, the FIM for the Phenanthrene contaminant has R^2 of 0.9681, showing a good fit while being less precise than the LIM with a higher R^2 value. The adsorption capacity, K_f, value (0.1388) is comparably lower to the LIM value of 1.0329 mg/g but comparable to that obtained from Quinoline-FIM, whereas the adsorption intensity, n, which characterizes the adsorption energy is 2.7691, demonstrating less favorable adsorption than Quinoline with n value of 4.292. Table 10 reveals that the Anthracene FIM has the lowest R^2 value of 0.9373, implying that it is less accurate in representing the sorption of Anthracene contaminant into the Zeolite surface. The Zeolite sorption capacity (K_f) for Anthracene contaminant is 0.1697 mg/g and the intensity of adsorption (n) is 3.5617, suggesting good adsorption, however, this model is less suited for the Anthracene adsorption process because of the lower R^2 and K_f values compared to the LIM's R^2, Qm values. As a result, while the FIM demonstrates favorable adsorption, it is less indicative of actual behavior for Quinoline, Anthracene, and Phenanthrene sorption processes at the Zeolite adsorption site. Furthermore, the R^2 value of 0.9885 obtained for Naphthalene in FIM indicates an excellent fit. The adsorption capacity (K_f) of 0.0051 is greater than that of LIM, and the n value of 3.8152 is greater than Phenanthrene and Anthracene but less than Quinoline adsorption intensity. This displays favorable adsorption, which demonstrates a heterogeneous surface adsorption is dominant (Thomas et al., 2010).

The Redlich-Peterson Isotherm Model (RIM): is a hybrid isotherm that can be used with both homogeneous and heterogeneous systems. R^2 is the coefficient of determination, while Kr (L/g) is the RIM constant. This constant is connected to adsorption capacity; larger values of Kr indicate greater adsorption capacity (Vasanth Kumar et al., 2010). aR (L/mg) is connected to adsorption energy, and g is the exponent parameter (0–1) that indicates the divergence from linearity. This exponent represents the heterogeneity of the adsorbent surface. When g = 1, the RIM simplifies to the LIM, suggesting that the adsorption sites are homogeneous. When g < 1, the adsorption process is heterogeneous, similar to the FIM. When g = 0, the adsorption capacity is constant independent of concentration (Vasanth Kumar et al., 2010). Table 10 shows an R^2 value of 0.9931 for Quinoline, which matches the LIM value, indicating a comparable fit. The adsorption capacity, Kr (0.032), and adsorption energy, aR (0.0661) for Quinoline are closely related to the LIM parameters, and the g value =1.000 indicates that the adsorption behavior is more consistent with the LIM, implying homogeneous adsorption. As a result, the LIM and RIM provide the greatest fit for the Quinoline contaminant, demonstrating that adsorption occurs mostly as a monolayer on a homogenous surface. In addition, the RIM for Phenanthrene, with an R^2 value of 0.9956, is equivalent to the LIM' R^2, with a Kr value of 0.0320, which closely aligns with LIM. However, the adsorption energy (aR) obtained from Quinoline-RIM is significantly larger than that of Phenanthrene-RIM (0.0331). The g value (0.9979) is close to one, emphasizing the resemblance to LIM behavior. The RIM for Anthracene has an R^2 value of 0.9895 and closely aligns with the LIM in terms of Kr (0.0388) and aR (0.0496). The g value (1.000) indicates that the adsorption is in the LIM pattern. The R^2 value of 0.9885 for Naphthalene matches that of FIMs, although the adsorption capacity (Kr) value (4.9901) and adsorption energy (aR) value (0.9788) differ significantly. The g value (0.7394) deviates

from one, indicating a more complex adsorption mechanism that differs from simple monolayer adsorption (LIM) but marginally resembles FIM.

The various isotherm plots in Figure 1 further reinforced these findings. We can observed that for Quinoline, Phenanthrene, and Anthracene, the isotherm traces of both LIM and RIM overlap while for Naphthalene, the isotherm plot of FIM and RIM overlaps. As a result, the LIM and RIM best characterize phenanthrene (Yakout et al., 2013; Balati et al., 2015; Saba et al., 2011), anthracene(Saba et al., 2011), and quinoline adsorption(Yang et al., 2019), indicating monolayer adsorption on a homogenous surface, but the FIM and RIM models better describe naphthalene sorption(Yakout et al., 2013). The Redlich-Peterson model has deviations for Naphthalene at g = 0.7394, implying that various adsorption mechanisms may be at work, making it more complex than other adsorbates.

Table 10: The Isotherm parameter values obtained from the Langmuir, Freundlich, and Redlich Peterson model for adsorbates

Isotherms model	**Langmuir parameters**			**Freundlich parameters**			**Redlich-Peterson parameter**			
Adsorbate	**R^2**	**Qm**	**K_L**	**R^2**	**Kf**	**n**	**R^2**	**Kr**	**aR**	**g**
Quinoline	0.9931	0.4870	0.0661	0.9519	0.1387	4.292	0.9931	0.032	0.0661	1.0000
Phenanthrene	0.9956	1.0329	0.0309	0.9681	0.1388	2.7691	0.9956	0.0320	0.0313	0.9979
Anthracene	0.9895	0.7829	0.0496	0.9373	0.1697	3.5617	0.9895	0.0388	0.0496	1.000
Naphthalene	0.9931	0.0208	0.0581	0.9885	0.0051	3.8152	0.9885	4.9901	0.9788	0.7394

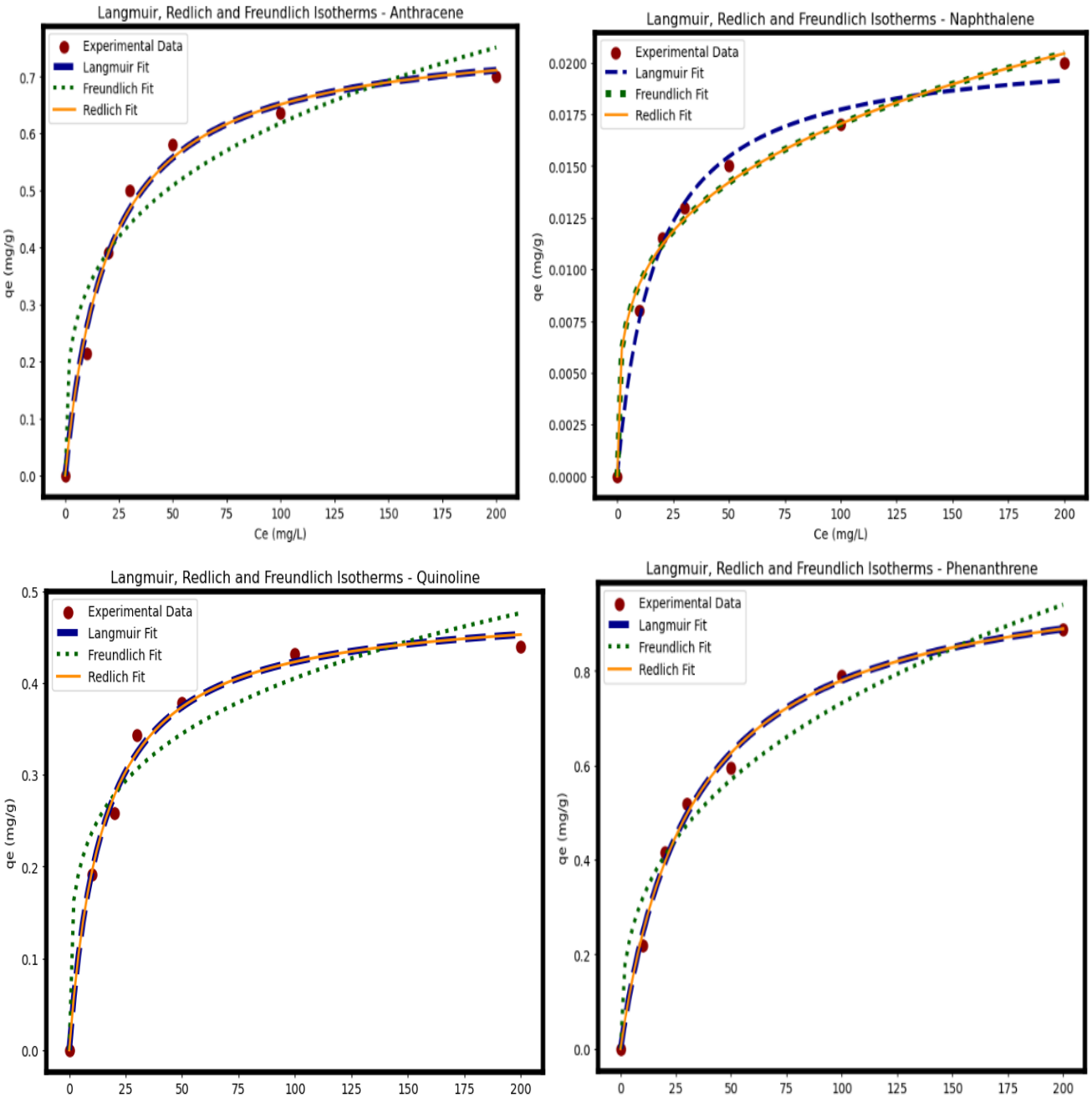

Figure 3: Isotherm plots for all the contaminant

4.0 CONCLUSION

The mass transfer studies conducted using batch kinetic experiments provided valuable insights into the sorption process of Naphthalene, Anthracene, Phenanthrene, and Quinoline in Water.

The findings establish mass transfer not as a peripheral factor, but as the central determinant of adsorption performance, governing contaminant transport, surface attachment, and pore diffusion.

The zeolite adsorbent featured a surface area of 74.92 m^2/g, a pore size of 4.000 Å, and a porosity of 0.59%,

creating extensive pore networks critical for internal diffusion. Mass transfer dynamics proved highly dependent on concentration. As initial concentrations rose from 10 to 200 g/L, equilibrium concentrations increased at rates varying by contaminant, revealing that molecular properties (size, polarity, structure) profoundly affect mass transfer resistance.

External diffusion model coefficients (K_f) decreased systematically with higher initial concentrations for all adsorbates reflecting a diminishing concentration gradient as the driving force. Anthracene showed superior mass transfer (K_f = 0.0540 m/s at 10 g/L), indicating minimal resistance moving to the zeolite surface. Conversely, quinoline exhibited the poorest behavior ($K_f = 5.60\times10^{-6}$ m/s at 200 g/L). The Furusawa and Smith model identified phenanthrene as having the highest boundary layer transport ($\beta L = 8.6\times10^{-5}$ m/s at 10 g/L). A modified version showed naphthalene's mass transfer coefficient dropped ~50% as concentration increased, suggesting its rate-limiting step is external movement to the surface.

Particle diffusion modeling revealed phenanthrene achieved exceptionally high diffusion coefficients ($De = 8.8\times10^{-4}$ m²/s at 30 g/L), indicating rapid pore transport where external mass transfer is the bottleneck. Biot number analysis (all values <100) confirmed that film mass transfer—movement through the stagnant boundary layer around zeolite particles is the predominant resistance for all contaminants. Phenanthrene exhibited the highest Bi values (40.98–57.11), confirming external resistance dominates, while the other three had Bi <40, where internal diffusion does not significantly lag.

Isotherm modeling connected mass transfer to equilibrium behavior. For quinoline, phenanthrene, and anthracene, Langmuir and Redlich-Peterson models indicated homogeneous monolayer adsorption a uniform surface after mass transfer overcomes boundary resistance. Naphthalene diverged, fitting the Freundlich model ($R^2 = 0.9885$), indicating heterogeneous surface adsorption with a range of binding energies.

Practical implications for water treatment are clear: since film mass transfer predominates, engineering should focus on reducing boundary layer thickness via turbulence or optimized flow. Distinct contaminant behaviors preclude a single optimal condition. The study's limitations include idealized single-solute conditions; real wastewater involves competitive effects. Future work should examine binary systems and hydrodynamic influences.

Compliance with ethical standards

This article does not contain any studies involving human or animal subjects.

Declaration of Competing Interests

The authors declare that they have no known competing financial interests or personal relationships that could have appeared to influence the work reported in this paper.

Credit authorship contribution statement

Alfred Daboh Yakubu: Conceptualization, Methodology, Investigation, Data curation, Writing – original draft, Writing – review & editing, Validation.

Evelyn Effi: Methodology, Writing – original draft, Writing –review & editing, Validation.

C.N Owabor: Supervision, Writing-review & editing, Validation.

Funding

This research did not receive any specific grant from funding agencies in the public, commercial, or not-for-profit sectors.

REFERENCES

1. Aguilera, P.; Gutiérrez-Ortiz, F. Prediction of fixed-bed breakthrough curves for H_2S adsorption: Importance of axial dispersion for design. *Chem. Eng. J.* **2016**, *289*, 93–98.
2. Bergman, T. L.; Lavine, A. S.; Incropera, F. P.; DeWitt, D. P. *Fundamentals of Heat and*

Mass Transfer, 7th ed.; Wiley: New York, 2011.
3. Bird, R. B.; Stewart, W. E.; Lightfoot, E. N. *Transport Phenomena*, 2nd ed.; Wiley: New York, 2006.
4. Cussler, E. L. *Diffusion: Mass Transfer in Fluid Systems*, 3rd ed.; Cambridge University Press: Cambridge, 2009.
5. Datta, C., Varun Kondra, T., Miller, M., & Streltsov, A. (2023). Catalysis of entanglement and other quantum resources. *Reports on Progress in Physics*, *86*(11), 116002.
6. Davila-Guzman, N. E.; Cerino-Córdova, F. J.; Soto-Regalado, E.; Loredo-Cancino, M.; Loredo-Medrano, J. A.; García-Reyes, R. B. A mass transfer model for the fixed-bed adsorption of ferulic acid onto a polymeric resin: Axial dispersion and intraparticle diffusion. *Environ. Technol.* **2016**, *37*, 1914–1922.
7. Elemile, O. O.; Akpor, B. O.; Ibitogbe, E. M.; Afolabi, Y. T.; Ajani, D. O. Adsorption isotherm and kinetics for nitrate removal using chicken feather fiber. *Cogent Eng.* **2022**, *9*, 2043227.
8. Gloc, M.; Mrozińska, Z.; Kudzin, M. H.; Kucińska-Król, I.; Paździor, K.; Olak-Kucharczyk, M. Adsorption of Cu(II) from real textile wastewater using natural and waste materials. *Appl. Sci.* **2026**, *16*, 905.
9. Ocampo-Pérez, R.; Aguilar-Madera, C. G.; Díaz-Blancas, V. 3D modeling of overall adsorption rate of acetaminophen on activated carbon pellets. *Chem. Eng. J.* **2017**, *321*, 510–520.
10. Odali, E. W., Iwegbue, C. M., Egobueze, F. E., Nwajei, G. E., & Martincigh, B. S. (2024). Distribution, sources, and risk of polycyclic aromatic hydrocarbons in soils from rural communities around gas flaring points in the Niger Delta of Nigeria. *Environmental Science: Processes & Impacts*, *26*(4), 721-733.
11. Sales, F. R. P., Serra, R. B. G., Figueirêdo, G. J. A. D., Hora, P. H. A. D., & Sousa, A. C. D. (2019). Wastewater treatment using adsorption process in column for agricultural purposes. *Revista Ambiente & Água*, *14*, e2178.
12. Udom, G. J., Niwamanya, N., Aziakpono, O. M., Udom, N. W. G., Malathi, H., Gupta, H., ... & Muzammil, K. (2025). Public health burden of polycyclic aromatic hydrocarbons in the East African environment: a systematic review. *Environmental Sciences Europe*, *37*(1), 145.
13. Wang, J.; Guo, X. Adsorption kinetic models: Physical meanings, applications, and solving methods. *J. Hazard. Mater.* **2020**, *390*, 122156.
14. Wang, J., & Guo, X. (2020). Adsorption kinetic models: Physical meanings, applications, and solving methods. *Journal of Hazardous materials*, *390*, 122156.